JOURNAL OF PHYSICAL ORGANIC CHEMISTRY
J. Phys. Org. Chem. 2004; **17:** 289–293
Published online 26 January 2004 in Wiley InterScience (www.interscience.wiley.com). DOI: 10.1002/poc.726

Effect of neighbouring amide group bulkiness on anchimerically assisted ether bond cleavage: Part 7

Antonio Arcelli,* Gianni Porzi,* Samuele Rinaldi and Sergio Sandri

Dipartimento di Chimica 'G. Ciamician', Via Selmi 2, Università di Bologna, 40126 Bologna, Italy

Received 2 June 2003; revised 15 October 2003; accepted 22 October 2003

ABSTRACT: The effect of the bulkiness of the amide group vicinal to the ether bond on the acid hydrolysis rate of substrates **1b–d** was investigated. The kinetic data showed that increased bulkiness of the acyl group has a considerable effect on the reaction rate, accelerating the anchimerically assisted hydrolytic process of the ether bond. A different mechanism is proposed for **1d**, which is supported by the thermodynamic activation parameters values. The hydrolysis rate of **1d** is about 3×10^5-fold higher than that of the reference compound. Copyright © 2004 John Wiley & Sons, Ltd.

KEYWORDS: anchimeric assistence; amides; ether cleavage; acid hydrolysis

INTRODUCTION

In a continuation of our program aimed at the acid-induced ether cleavage anchimerically assisted by a vicinal amide group,[1–6] we have investigated the effect on the hydrolytic process induced by the change of the R acyl group of the substrate **1** (Scheme 1).

The compounds previously studied, i.e. **1** [R═CH_3 (Ref. 1) or Ph (Ref. 3)], showed that the proton concentration does not have a constant effect on the reaction rate. In fact, at all the temperatures investigated the plots of the pseudo-first-order rate constant (k_{obs}) vs [HCl] showed two practically linear regions with different slopes. Below 5 M HCl the acidity increase causes a relatively small increase in k_{obs}, while a clearly greater reaction sensitivity to [H^+] is observed above 5 M HCl. We deduced that the greater slope of the plot of k_{obs} vs [HCl] at acidity values higher than 5 M HCl, is ascribable to a strong increase in the activity coefficient ratio ($f_{SH^+}/f^{\neq}$) at ionic strengths $I > 5$ M.[3,6]

To investigate the effect of the bulkiness of the amide group vicinal to the ether bond on the acid hydrolysis rate, we have extended the kinetic studies to the substrates **1b–d** synthesized following the procedure described previously for analogous compounds.[1,3]

RESULTS AND DISCUSSION

We report the kinetic measurements accomplished at various temperatures and in the acidity range 4.9–8.6 M HCl, where the plot of the rate constant (k_{obs}) vs [HCl] is practically linear, as previously observed also for similar substrates.[1,3]

From the rate constants (k_{obs}), calculated by measuring the optical density vs time, for the acid-catalysed hydrolysis of **1b–d** under various experimental conditions (Table 1), the thermodynamic activation parameters were calculated at 50 °C (Table 2) from the linear relationship of $\ln k_{H^+}$ vs $1/T$, where k_{H^+} is obtained from the slope of the plot of k_{obs} vs [H^+] for each temperature (Table 1). The relative rates, calculated at 57.8 °C from k_{H^+} values, for **1a**, **1b**, **1c** and **1d** are 1:3.5:12:137, respectively. Thus, the point which clearly emerges is that increased bulkiness of the acyl group has a considerably effect on the reaction rate, accelerating the anchimerically assisted hydrolytic process, which is unexpectedly high for the substrate **1d**.

In order to realize the effect of the acyl substituent on the reaction rate, the logarithm of the second-order rate constants at 57.8 °C were plotted against the ν^* values calculated by Charton,[7] these parameters taking into account the steric effect of the branching of the alkyl group. For the substrate **1d** we observed a meaningful positive deviation from the expected value calculated from the equation $\log k_{H^+} = (2.38 \pm 0.02)\nu^* - (5.47 \pm 0.02)$, which fits very well ($r = 0.9999$ and $F = 14\,260$) the other substrates (Fig. 1). A similar linear correlation for **1a–c**, but with a negative slope, was found also between $\log k_{H^+}$ and the Taft parameter σ^* (not reported). Further, it should be emphasized that an analogous very good linear correlation between the pK_{SH^+} values (determined as reported in the Experimental section) and ν^* was found for **1a–c**, whereas the pK_{SH^+} of **1d** showed a considerable deviation also in this case (Fig. 2).

**Correspondence to:* A. Arcelli and G. Porzi, Dipartimento di Chimica 'G. Ciamician', Università di Bologna, Via Selmi 2, 40126 Bologna, Italy.
E-mail: porzi@ciam.unibo.it
Contract/grant sponsor: University of Bologna.

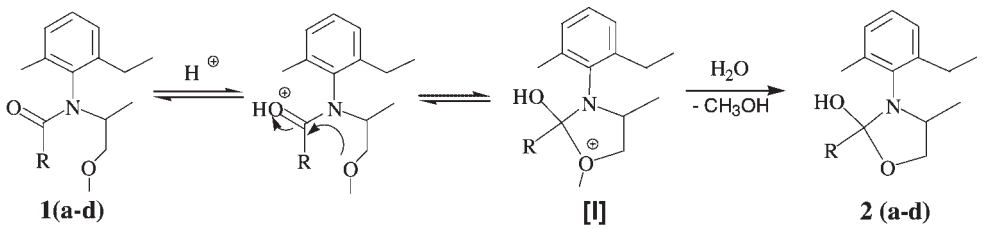

Scheme 1. R = (**1a**) CH_3; (**1b**) C_2H_5; (**1c**) $CH(CH_3)_2$; (**1d**) $C(CH_3)_3$

We believe that the rate increase observed on going from **1a** to **1d** is not ascribable to the steric acceleration effect (found, for instance, in elimination reactions[8]) because, from the ground state to the transition state, a crowding effect occurs at the carbonyl carbon atom. In fact, in the course of the reaction, the electronic character of the carbonyl carbon changes from sp^2 to sp^3, hence the increasing bulkiness of the amide function should reduce its reactivity owing to the increased crowding in the transition state. In contrast, for the investigated amides **1a–d** the reverse is true, i.e. the more crowded substrate (**1d**) showed a higher reactivity. We believe that the rate decrease on going from **1d** to **1a** is probably due to the hyperconjugative effect[9] of α-hydrogens to the carbonyl, i.e. an increase in the number of these hydrogens causes a decrease in the observed rate constant. Actually, the replacement of a hydrogen atom with a CH_3 group has a destabilizing effect on the protonated substrate with respect to the transition state giving rise to a decrease in the activation energy.

Table 1. Rate constants and experimental conditions for the acid hydrolysis of **1b–d**

$T \pm 0.1$ (°C)	[HCl] (mol dm^{-1}) (a)[a]	$10^3 k_{obs}$(s^{-1})		
		1b	**1c**	**1d**
31.1	5.95			0.61
	7.52			1.62
	8.71			2.56
36.6	4.97			0.50
	5.94			1.27
	7.50			3.28
	8.69			4.98
45.5	4.95		0.06	1.78
	5.92		0.25	3.63
	7.46		0.64	9.54
	8.65		0.90	13.00
50.2	4.93			2.67
	5.90			7.56
	7.45			14.00
	8.63			19.30
52.3	4.93	0.126		
	5.90	0.222		
	7.31	0.389		
	8.57	0.558		
55.5	4.96		0.33	
	6.20		0.80	
	7.40		1.80	
	8.64		2.54	
57.8	4.92	0.275	0.364	6.70
	5.89	0.51	1.20	15.30
	7.43	0.865	2.10	27.00
	8.60	1.07	3.20	38.30
60.1	4.96	0.33	0.60	
	6.19	0.55	1.23	
	7.39	1.00	2.47	
	8.61	1.30	3.83	
65.1	4.94		1.06	
	6.17		1.82	
	7.37		4.14	
	8.58		5.93	
70.2	4.89	1.06		
	5.86	1.42		
	7.24	3.24		
	8.49	3.36		
79.2	4.87	2.19		
	5.83	2.96		
	7.21	5.71		
	8.46	7.10		

[a] Values corrected at the various temperatures.[1]

By plotting $\Delta H^{\neq}$ vs $\Delta G^{\neq}$ of **1a–d** in a statistical weight-meaningful form, for **1d** a significant positive deviation from the linear regression concerning the isokinetic relationship (IKR) was observed (Fig. 3). Because a linear relationship between $\Delta H^{\neq}$ and $\Delta G^{\neq}$ generally means that only one reaction mechanism is present, the observation of significant scattering could suggest that **1d** reacts by a different mechanism[10,11] to the other substrates investigated.

Similarly, the rate increase (about 3.2-fold) for **1d** with respect to the expected value suggests the same hypothesis. This is in agreement with the lower acidity of the conjugate acid of **1d** ($pK_{SH^+} = -3.35$) compared with the value extrapolated from the correlation in Fig. 2 ($pK_{SH^+} = -4.22$). This suggests that the protonation mainly occurs at the ether position, probably owing to the increased steric interference of the *tert*-butyl group with solvation.[12]

With this mechanistic hypothesis, the carbonyl oxygen atom would perform a nucleophilic attack on the carbon adjacent to the protonated —OCH_3 fragment. This would lead to the expulsion of a CH_3OH molecule (Scheme 2). This attack should occur with a higher rate, as indicated by the activation parameters in Table 2. We believe that this mechanism gives a sterically less strained transition state. In fact, the intermediate **II** is a five-membered cyclic carbocation where the angle between the *tert*-butyl carbon atom and N is 120°, i.e. greater than in the five-membered cyclic oxonioun intermediate **I** proposed in the mechanism described in Scheme 1.

Table 2. Thermodynamic activation parameters for the acid hydrolysis of **1a–d**[a]

Substrate **1**	$\Delta G^{\neq}$ (kcal mol^{-1})	$\Delta H^{\neq}$ (kcal mol^{-1})	$\Delta S^{\neq}$ (cal mol^{-1} K^{-1})	$T\Delta S^{\neq}$ (kcal mol^{-1})
(**1a**) R = CH_3[b]	25.8 ± 1.5	23.3 ± 1.0	−7.6 ± 3.2	−2.5 ± 1.0
(**1b**) R = C_2H_5	24.9 ± 0.7	20.5 ± 0.5	−13.5 ± 1.6	−4.4 ± 0.5
(**1c**) R = $CH(CH_3)_2$	24.1 ± 0.5	19.0 ± 0.4	−15.7 ± 1.1	−5.1 ± 0.4
(**1d**) R = $C(CH_3)_3$	22.4 ± 0.7	18.1 ± 0.5	−13.4 ± 1.6	−4.3 ± 0.5

[a] Calculated at 50°C from the k_{H^+} values.
[b] From kinetic data reported in Ref. 1.

This hypothesis is strengthened by the ΔS value of **1d** in comparison with **1c**. The $\Delta G^{\neq}$ decrease for **1d** with respect to **1c** is due to an increase in both $\Delta H^{\neq}$ (0.9 kcal mol^{-1}) and $T\Delta S^{\neq}$ (0.8 kcal mol^{-1}) (1 kcal = 4.184 kJ). In contrast, the $\Delta G^{\neq}$ decrease on going from **1a** to **1c** is exclusively due to the $\Delta H^{\neq}$ increase, the $T\Delta S^{\neq}$ increase (from −2.5 to 5.1 kcal mol^{-1}) being unfavourable.

The reaction path in Scheme 2 should be favoured over that in Scheme 1 because in the former case the intermediate **II** which forms in the rate-determining step is clearly stabilized by resonance. The intermediate **II** can be described by three resonance structures which indicate that the positive charge is delocalized among sp^2 carbon, oxygen and nitrogen atoms and that the intermediate has a tertiary carbocation character. Conversely, a similar stabilization cannot be recognized in intermediate **I**, where the positive charge is frozen on the oxygen atom.

The cross-over from the mechanism in Scheme 1 to that in Scheme 2 can be ascribed at least in part to the different protonation of substrate **1d** in comparison with **1a–c**. However, we do not exclude the possibility that the mechanism in Scheme 2 can operate also with the **1c** derivative, at least in part.

In conclusion, we believe that the relevant rate increase observed on going from **1a** to **1d** can be reasonably ascribed to the hyperconjugative effect on the protonated substrate (i.e. the reacting species). For **1d** the increase in the steric hindrance near to the C═O is an important factor which favours the change in the reaction mechanism.

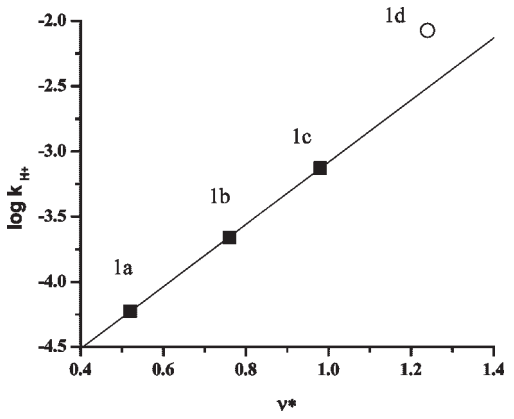

Figure 1. Log k_{H^+} (mol^{-1} s^{-1}) vs ν^* for the acid hydrolysis of **1a–c** at 57.8 °C

We emphasize that the effectiveness of the neighbouring amide group assistance in the acid hydrolysis of **1d** is remarkable. In fact, the ratio between the second-order rate constants (k_{H^+}) of **1d**, calculated at 69.9 °C from thermodynamic activation parameters, and of the reference compound without the amide function, already reported,[1] is about 3×10^5.

EXPERIMENTAL

General

^{1}H and ^{13}C NMR spectra were recorded with a Varian Gemini 300 (300 MHz) instrument using $CDCl_3$ as solvent. Chemical shifts are in ppm relative to $CDCl_3$ and the coupling constants (J) are in hertz. UV spectra and kinetic measurements were recorded on a Perkin-Elmer Lambda 6 spectrophotometer. IR spectra were recorded on a Nicolet 210 spectrophotometer.

The products were analysed by using a Hewlett-Packard Model 1100 liquid chromatograph–single-quadrupole mass-selective detector system, with an atmospheric pressure chemical ionization–electrospray interface, using a Zorbax Eclipse XDB-C8 column.

Products

*General procedure for the synthesis of **1b–d**.* The products were obtained starting from 6-ethyl-*o*-toluidine and

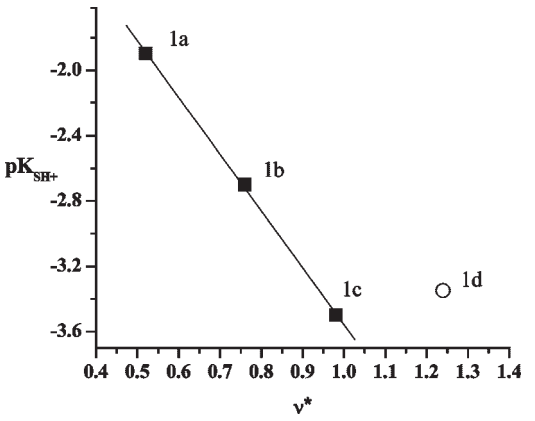

Figure 2. pK_{SH^+} of **1a–c**, at 25 °C vs ν^*

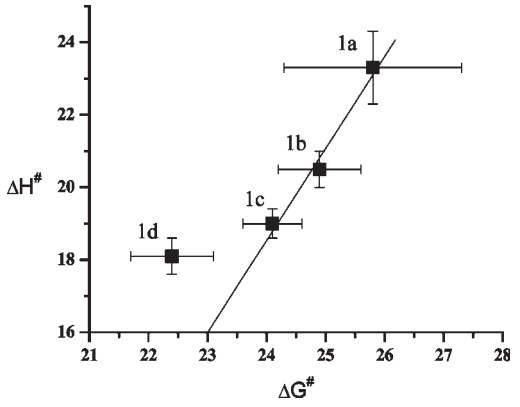

Figure 3. $\Delta H^{\neq}$ vs $\Delta G^{\neq}$ (kcal mol^{-1}) for the acid hydrolysis of **1a–c**

(±)-ethyl 2-bromopropionate and following the procedure already used to synthesize the analogous substrate **1a**.[3] After purification by silica gel chromatography, eluting with hexane–ethyl acetate, the pure products were isolated as an oil in 65–70% overall yield.

*N-(2-Ethyl-6-methylphenyl)-N-(methoxyprop-2-yl)propanamide (**1b**).* ^{1}H NMR, δ 1.0 (t, 3H, $J = 7.4$); 1.05–1.15 (2d, 3H, $J = 5$); 1.25 (t, 3H, $J = 7.5$); 1.8 (m, 2H); 2.2 (2s, 3H); 2.5 (m, 2H); 3.3 (2s, 3H); 3.45 (2dd, 1H, $J = 7.2$, 9.3); 3.65–3.8 (2dd, 1H, **J** = 3.9, 9.3); 4.25 (m, 1H); 7.12 (m, 3ArH). ^{13}C NMR, δ 8.9, 13.6, 13.9, 15.3, 15.5, 18.5, 23.2, 23.5, 27.5, 27.6, 53.7, 53.9, 58.1, 74.9, 126.1, 126.2, 127.7, 128.2, 136.5, 136.6, 138.3, 142.1, 142.2, 174.1. IR (thin film): $\nu = 1659.8\,\text{cm}^{-1}$ (C═O). HPLC–MS: *m/z* 264.2 ($M^+ + 1$), 286.2 ($M^+ + \text{Na}$).

*N-(2-Ethyl-6-methylphenyl)-N-(methoxyprop-2-yl)-2-methylpropanamide (**1c**).* ^{1}H NMR, δ 0.95 (m, 6H); 1.05–1.15 (2d, 3H, $J = 7$); 1.23 (m, 3H); 2.1 (m, 1H); 2.2 (2s, 3H); 2.55 (m, 2H); 3.25–3.3 (2s, 3H); 3.5 (dd, 1H, $J = 8.7$, 9.3); 3.65–3.8 (2dd, 1H, $J = 3.9$, 9.3); 4.1 (m, 1H); 7.1 (m, 3ArH). ^{13}C NMR, δ 13.6, 14, 15.4, 15.7, 18.7, 18.9, 19, 19.5, 19.6, 19.7, 19.8, 23.3, 23.5, 32, 54.3, 54.6, 58.3, 75.1, 126, 126.2, 127.7, 127.8, 128.4, 136.5, 136.7, 138.7, 142.2, 142.3, 178.4. IR (thin film): $\nu = 1655.8\,\text{cm}^{-1}$ (C═O). HPLC–MS: *m/z* 278.2 ($M^+ + 1$), 300.2 ($M^+ + \text{Na}$).

*N-(2-Ethyl-6-methylphenyl)-N-(methoxyprop-2-yl)-2,2-dimethylpropanamide (**1d**).* ^{1}H NMR, δ 0.92 (s, 9H); 1.08–1.15 (2d, 3H, $J = 7$); 1.25 (2t, 3H, $J = 7.2$); 2.2–2.3 (2s, 3H); 2.6 (m, 2H); 3.3 (2s, 3H); 3.55 (2dd, 1H, $J = 7.4$, 9.3); 3.7 (2dd, 1H, $J = 3.6$, 9.3); 3.95 (m, 1H); 7.1 (m, 3ArH); ^{13}C NMR, δ 13.4, 13.8, 15.3, 15.6, 19.2, 19.4, 23.7, 29, 29.1, 41.6, 41.7, 56.9, 57.5, 58.4, 75.5, 75.6, 125.7, 125.8, 127.7, 127.8, 128, 128.1, 136.9, 137.3, 140, 140.1, 142.5, 142.7, 178.7, 178.8. IR (thin film): $\nu = 1634.6\,\text{cm}^{-1}$ (C═O). HPLC–MS: *m/z* 292.2 ($M^+ + 1$), 314.2 ($M^+ + \text{Na}$).

*3-(2-Ethyl-6-methylphenyl)-2-ethyl-2-hydroxy-4-methyloxazolidine (**2b**).* This it was obtained by subjecting **1b** to hydrolysis in 5 M HCl at 80 °C. After about 1 h, the reaction mixture was evaporated to dryness *in vacuo* and the oily residue was pure by TLC analysis. ^{1}H NMR, δ 1 (t, 3H, $J = 7.4$); 1.1–1 .2 (2d, 3H, $J = 6.6$); 1.25 (t, 3H, $J = 7.6$); 1.8 (m, 2H); 2.2 (2s, 3H); 2.4–2.65 (m, 2H); 3.62 (m, 1H); 4–4.25 (m, 2H); 7.05–7.4 (m, 3ArH). ^{13}C NMR, δ 8.8, 13.5, 14, 14.8, 15, 18.4, 18.7, 23.4, 27.5, 46.8, 46.9, 56.1, 56.6, 126.4, 128, 128.5, 135.9, 136.2, 137.8, 141.7, 141.8, 174.2, 174.3. IR (thin film): $\nu = 3440\,\text{cm}^{-1}$ (broad, OH). HPLC–MS: *m/z* 250.2 ($M^+ + 1$), 272.2 ($M^+ + \text{Na}$).

*3-(2-Ethyl-6-methylphenyl)-2-hydroxy-2-isopropyl-4-methyloxazolidine (**2c**).* This was obtained by subjecting **1c** to hydrolysis in 5 M HCl at 70 °C for about 2 h. The reaction mixture was evaporated to dryness *in vacuo* and the oily residue was pure by TLC analysis. ^{1}H NMR, δ 0.97 (m, 6H); 1.25 (m, 6H); 2–2.25 (m, 1H); 2.2–2.3 (2s, 3H); 2.55 (m, 2H); 3.7 (m, 1H); 3.95–4 .2 (m, 2H); 7.15 (m, 3ArH). ^{13}C NMR, δ 13.7, 14.2, 15.1, 15.4, 19, 19.2, 19.5, 19.7, 19.8, 19.9, 23.6, 32.1, 47.3, 57.1, 57.7, 57.8, 126.5, 126.6, 128, 128.2, 128.3, 128.8, 136.5, 138.4, 142, 142.1, 178.6. IR (thin film): $\nu = 3459\,\text{cm}^{-1}$ (broad, OH). HPLC–MS: *m/z* 264.2 ($M^+ + 1$), 286.2 ($M^+ + \text{Na}$).

*3-(2-Ethyl-6-methylphenyl)-2-hydroxy-4-methyl-2-tert-butyloxazolidine (**2d**).* This was obtained by subjecting **1d** to hydrolysis in 5 M HCl at 60 °C for about 0.5 h. The reaction mixture was evaporated to dryness *in vacuo* and the oily residue was pure by TLC analysis. ^{1}H NMR, δ 1.2 (3s, 9H); 1.3–1.35 (2t, 3H, $J = 7.4$); 1.44 (2d, 3H, $J = 6.5$); 2.35–2.45 (2s, 3H); 2.52–2 .82 (m, 1H); 4.95 (m, 1H); 5.1–5.35 (m, 1H); 5.9 (m, 1H); 7.3 (m, 3ArH). ^{13}C NMR, δ 13.3, 14, 15.4, 15.9, 18.4, 19.2, 23.4, 23.7,

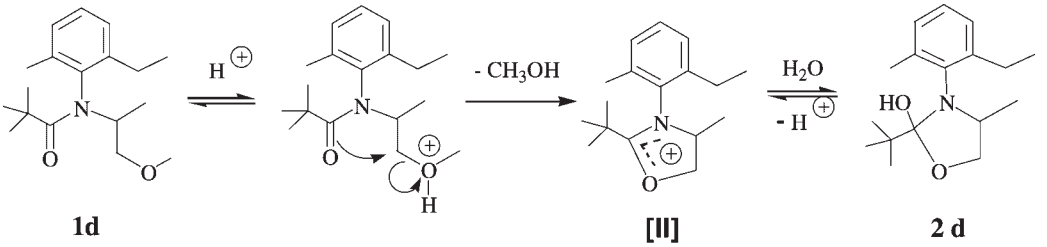

Scheme 2

26.9, 36.8, 36.9, 64, 64.9, 77.2, 126.6, 127.2, 129, 129.1, 129.3, 129.4, 130.8, 134.1, 135.2, 140, 140.7, 182.8. IR (thin film): $\nu = 3465\ cm^{-1}$ (broad, OH). HPLC–MS: *m/z* 278.2 ($M^+ + 1$), 300.2 ($M^+ + Na$).

Kinetic experiments

The acid hydrolysis was followed spectrophotometrically, as described previously,[3] by measuring the change in optical density (OD) at 266 nm for substrates **1b** and **1c** and at 240 nm for **1d**. The reactions follow a pseudo-first-order law over at least 90% of reaction. The kinetics were measured in duplicate runs and the mean value was reported. The rate constants (k_{obs}) were obtained from the equation $OD_t = OD_0 + (OD_\infty - D_0)[1 - \exp(-tk_{obs})]$ by plotting at least 200 values of OD with a non-linear least-squares routine (FigP6.0 program, Biosoft) and very good to excellent plots were always obtained. After completion of the reaction, after about 10 half-lives, the products were identified by mass spectrometry by comparison with reference compounds **2b–d** obtained as reported above.

pK_{SH^+} measurement

The pK_{SH^+} values of substrates **1b–d** were measured spectrophotometrically at 25 °C in HCl solutions following the protocol reported previously.[3] The OD values of protonated species were measured in 10 M HCl. Since the hydrolysis of **1d** proceeds significantly also at room temperature, the absorbance was recorded as a function of time and extrapolated to $t = 0$. The pK_{SH^+} values, calculated from the equation $pK_{SH^+} = H_0 + n\log([SH^+]/[S])$, are −2.7 ($n = 0.74$) for **1b**, −3.5 ($n = 0.41$) for **1c** and −3.35 ($n = 1.82$) for **1d**.

Acknowledgement

Financial support from the University of Bologna, 'Ricerca fondamentale orientata' (ex. 60%) is gratefully acknowledged.

REFERENCES

1. Arcelli A, Porzi G, Sandri S. *Tetrahedron* 1995; **51**: 9729–9736 and references cited therein.
2. Arcelli A, Papa M, Porzi G, Sandri S. *Tetrahedron* 1997; **53**: 10513–10516.
3. Arcelli A, Porzi G, Rinaldi S, Sandri S. *J. Chem. Soc., Perkin Trans. 2* 2001; 296–301.
4. Arcelli A, Cecchi R, Porzi G, Rinaldi S, Sandri S. *Tetrahedron* 2001; **57**: 4039–4043.
5. Arcelli A, Cecchi R, Porzi G, Rinaldi S, Sandri S. *Tetrahedron* 2001; **57**: 6843–6846.
6. Arcelli A, Paradisi F, Porzi G, Rinaldi S, Sandri S. *J. Chem. Res.* 2002; *(S)* 199, (M) 501.
7. Charton M. *J. Org. Chem*. 1979; **44**: 903–906.
8. Chuchani G, Dominguez RM. *Int. J. Chem. Kinet.* 1981; **13**: 577–589.
9. Grob CA, Rich R. *Tetrahedron Lett.* 1978; **7**: 663–666, and references cited therein.
10. Linert W. *Chem. Soc. Rev.* 1989; **18**: 477–555.
11. Linert W. *Chem. Soc. Rev.* 1994; **23**: 429–438.
12. Lowry TH. Schueller Richardson K. *Mechanism and Theory in Organic Chemistry*. Harper and Row: New York, 1987; 308.